A bimodular theory for finite deformations: comparison of orthotropic second-order and exponential stress constitutive equations for articular cartilage

Stephen M. Klisch - California Polytechnic State University, San Luis Obispo

Abstract Cartilaginous tissues, such as articular cartilage and the annulus fibrosus, exhibit orthotropic behavior with highly asymmetric tensile–compressive responses. Due to this complex behavior, it is difficult to develop accurate stress constitutive equations that are valid for finite deformations. Therefore, we have developed a bimodular theory for finite deformations of elastic materials that allows the mechanical properties of the tissue to differ in tension and compression. In this paper, we derive an orthotropic stress constitutive equation that is second-order in terms of the Biot strain tensor as an alternative to traditional exponential type equations. Several reduced forms of the bimodular second-order equation, with six to nine parameters, and a bimodular exponential equation, with seven parameters, were fit to an experimental dataset that captures the highly asymmetric and orthotropic mechanical response of cartilage. The results suggest that the bimodular second-order models may be appealing for some applications with cartilaginous tissues.

1 Introduction

The work in this paper is motivated by the difficulty of, and the need for, developing accurate stress constitutive equations for fiber-reinforced cartilaginous tissues. Cartilage is composed of chondrocytes embedded in an extracellular matrix consisting primarily of proteoglycans, a crosslinked collagen network, and water. The proteoglycans are negatively charged molecules that mainly resist compressive loads (Basser et al. 1998; Lai et al. 1991) while the collagen network primarily resists tensile and shear loads (Mow and Ratcliffe 1997; Venn and Maroudas 1977). Due to this molecular structure, articular cartilage typically exhibits a mechanical response with marked anisotropy and tension–compression asymmetry (Akizuki et al. 1986; Laasanen et al. 2003; Soltz and Ateshian 2000; Wang et al. 2003; Woo et al. 1976, 1979), and likely experiences finite, multi-dimensional strains due to typical in vitro and in vivo loads. Although MRI measurements of in situ and in vivo joints have predicted that cartilage is subject to average strains of less than 10% under physiologic loading conditions (Eckstein et al. 2000; Herberhold et al. 1999), local strains may be much higher due to nonhomogeneous mechanical properties that depend on both anatomic location (Laasanen et al. 2003) and depth from the articular surface (Schinagl et al. 1997; Wang et al. 2001). For physiologic loading conditions, FEM contact analyses (Donzelli et al. 1999; Krishnan et al. 2003) suggest that in situ cartilage may experience local strains up to 26%, suggesting that the tissue is in the nonlinear range of its stress–strain relationship (Huang et al. 1999).

Due to the complex mechanical behavior of cartilaginous tissues, the development of accurate finite deformation models of the equilibrium elastic response has been difficult. Lotz and colleagues developed an orthotropic finite deformation model for the annulus fibrosus using an exponential strain energy function; however, maximum errors between the theoretical and experimental stresses in uniaxial tension (UT) were approximately 50% (Klisch and Lotz 1999; Wagner and Lotz 2004). For articular cartilage, there has been no finite deformation model presented that accurately describes its orthotropic response for multiple experimental protocols including tension and compression. However, an elastic stress constitutive equation for finite deformations has been used in more complex models, including multiphasic models with isotropic (Ateshian et al. 1997; Holmes and Mow 1990; Kwan et al. 1990) and transversely isotropic (Almeida and Spilker 1997) material symmetry.

For infinitesimal strains, Ateshian and colleagues (Soltz and Ateshian 2000; Wang et al. 2003) have employed elastic and biphasic models with a bimodular stress constitutive equation that allows for different mechanical properties in tension and compression. Their model can describe the mechanical response in unconfined compression in three

orthogonal directions while providing reasonable predictions for the other protocols (Wang et al. 2003). Those models were based on a bimodular theory for infinitesimal strains (Curnier et al. 1995) in which the material constants may be discontinuous (or jump) across a surface of discontinuity in strain space, provided that the stress continuity conditions are satisfied at the surface. Recently, several exponential models for finite deformations that allow for different mechanical properties in tension and compression have been used for the arterial wall (Holzapfel et al. 2004) and the annulus fibrosus (Baer et al. 2004). One reason that an exponential strain energy function is often used may be due to its ability to model the highly asymmetric tension–compression response without invoking the bimodular feature (Almeida and Spilker 1997; Klisch and Lotz 1999; Wagner and Lotz 2004).

Our long-term goal is to develop an accurate stress–strain equation that can simultaneously describe the equilibrium elastic response in tension, confined and unconfined compression, and torsional shear. Accurate stress constitutive equations for cartilaginous tissues have practical applications. They may be used in FEMs of in vivo joints; the results of Donzelli et al. (1999) and Krishnan et al. (2003) suggest that more accurate stress constitutive equations for large deformations may lead to an improved understanding of cartilage degeneration and failure. They may be used in microstructural finite element models to estimate the mechanical microenvironment of the cell in order to improve our understanding of the mechanotransduction process (Baer et al. 2004; Guilak and Mow 2000). Also, accurate stress constitutive equations are needed for conducting robust validation tests of the cartilage growth mixture models that we have developed (Klisch et al. 2000, 2001, 2003, 2005; Klisch and Hoger 2003) and to estimate how the mechanical properties of cartilage evolve during growth using these models.

In this study, we hypothesize that a bimodular second-order stress constitutive equation can be used to accurately model the anisotropic and asymmetric tensile–compressive response of articular cartilage. The specific objectives are to:

(1) derive a general bimodular theory for finite deformations;
(2) derive a bimodular second-order stress constitutive equation for orthotropic materials; and
(3) compare the predictive capability of several bimodular second-order models and a bimodular exponential model using experimental data gathered from the literature.

In the Discussion, we present ongoing aims that relate to the integration of the derived phenomenological model with microstructurally based models.

2 Methods

In this section, we outline the derivation of a second-order stress constitutive equation for orthotropic materials. Then, we propose a general theory for bimodular elastic materials and, consequently, derive a bimodular second-order stress constitutive equation. Finally, we study the abilities of bimodular second-order and exponential models to describe the mechanical response of articular cartilage in uniaxial tension (UT) and confined compression (CC).

2.1 Background

The deformation gradient tensor $\mathbf{F}$ is uniquely decomposed by the polar decomposition theorem as

$$\mathbf{F} = \mathbf{RU}, \tag{1}$$

where $\mathbf{R}$ is a proper-orthogonal tensor and the right stretch tensor $\mathbf{U}$ is a symmetric positive-definite tensor. The Biot strain tensor $\mathbf{E}$ and the right Cauchy–Green deformation tensor $\mathbf{C}$ are

$$\mathbf{E} = \mathbf{U} - \mathbf{I}, \quad \mathbf{C} = \mathbf{F}^{\mathrm{T}}\mathbf{F}, \tag{2}$$

where the superscript T signifies the transpose operator. The Cauchy and first Piola–Kirchhoff stress tensors (denoted as $\mathbf{T}$ and $\mathbf{P}$, respectively) are related by

$$J\mathbf{T} = \mathbf{P}\mathbf{F}^{T}, \tag{3}$$

where J is the determinant of $\mathbf{F}$. The stress constitutive equations for a Green-elastic material may be expressed as

$$\mathbf{P} = 2\mathbf{F}\frac{\partial W}{\partial \mathbf{C}} = 2\mathbf{F}\sum_{i=1}^{n}\frac{\partial W}{\partial I_i}\frac{\partial \mathbf{I}_i}{\partial \mathbf{C}}, \tag{4}$$

where W is a scalar strain energy function that depends on a set of invariants of $\mathbf{C}$, $I_{\mathrm{C}} = \{I_{\mathrm{i}}(\mathbf{C}); i = 1, n\}$, corresponding to the material symmetry group:

$$W = \hat{W}(\mathbf{C}) = \tilde{W}(I_1(\mathbf{C}), I_2(\mathbf{C}), ..., I_n(\mathbf{C})) \equiv \tilde{W}(I_C). \tag{5}$$

In the second-order theory, an alternative form of the stress constitutive equation for a Green-elastic material is used:

$$\mathbf{T} = \mathbf{R}\hat{\mathbf{T}}(\mathbf{U})\mathbf{R}^{T} = \mathbf{R}\tilde{\mathbf{T}}(\mathbf{E})\mathbf{R}^{T}, \quad \mathbf{P} = \mathbf{R}\hat{\mathbf{P}}(\mathbf{U}) = \mathbf{R}\tilde{\mathbf{P}}(\mathbf{E}), \tag{6}$$

where the functions $\hat{\mathbf{T}}(\mathbf{U})$ and $\hat{\mathbf{P}}(\mathbf{U})$ are derived from W:

$$W = \hat{W}(\mathbf{U}) = \tilde{W}(I_1(\mathbf{U}), I_2(\mathbf{U}), ..., I_n(\mathbf{U})) \equiv \tilde{W}(I_U) \tag{7}$$

and $I_U = \{I_i(\mathbf{U}); i = 1, n\}$ is the set of basic polynomial invariants of $\mathbf{U}$ corresponding to the material symmetry group.

2.2 Second-order orthotropic materials

For isotropic elastic materials, various second-order theories for Green-elastic materials have been proposed using different strain tensors (Hoger 1999; Murnaghan 1937, 1951; Rivlin 1953) which differ depending on which strain tensor is used (Ogden 1984). In this paper, the Biot strain tensor is used in the second-order equations for two reasons. First, it has a clear physical interpretation; the eigenvalues of the Biot strain tensor represent the principal extensions. Second, the results of Van Dyke and Hoger (2000) suggested that the second-order stress equations using the Biot strain tensor, as compared to other strain measures, provided a better approximation of the exact solutions to a group of boundary-value

problems using specific nonlinear elastic materials. For an arbitrary material symmetry group, general stress constitutive equations that are second-order in terms of the Biot strain tensor have been presented (Hoger 1999). Those equations are presented in Appendix A [see (27) and (28)]. Explicit stress constitutive equations were obtained only for isotropic and transversely isotropic materials in Hoger (1999); consequently, the derivation for orthotropic materials was one aim of the present work.

For orthotropic materials, we assume that the material symmetry group includes reflections about three planes defined by a set of three basis vectors $(\mathbf{E}_1, \mathbf{E}_2, \mathbf{E}_3)$. Structural tensors $(\mathbf{M}_1, \mathbf{M}_2, \mathbf{M}_3)$ are defined as

$$\mathbf{M}_1 = \mathbf{E}_1 \otimes \mathbf{E}_1, \quad \mathbf{M}_2 = \mathbf{E}_2 \otimes \mathbf{E}_2, \quad \mathbf{M}_3 = \mathbf{E}_3 \otimes \mathbf{E}_3, \tag{8}$$

where $\otimes$ is the tensor dyadic product. We use the set of invariants

$$\begin{aligned}\{I_i(\mathbf{U})\} = \{&\mathbf{M}_1\cdot\mathbf{U}, \mathbf{M}_1\cdot\mathbf{U}^2, \mathbf{M}_2\cdot\mathbf{U}, \mathbf{M}_2\cdot\mathbf{U}^2,\\ &\mathbf{M}_3\cdot\mathbf{U}, \mathbf{M}_3\cdot\mathbf{U}^2, \mathrm{I}\cdot\mathbf{U}^3\}\\ \equiv\ &\{I_1, I_2, I_3, I_4, I_5, I_6, I_7\}.\end{aligned} \tag{9}$$

In Appendix B, we outline the derivation of the general orthotropic second-order stress constitutive equation. However, that general equation has 46 material constants and is not practical for use. Although we initially derived the necessary conditions for stress continuity postulated in the bimodular theory for that general equation, here we first obtain a reduced model for the second-order orthotropic stress constitutive equation.

To obtain a reduced model, we make the following assumptions regarding the dependence of the strain energy function W (7) with respect to the invariants $I_i(\mathbf{U})$ (9):

(i) W is independent of $\{I_2,\ I_4,\ I_6\}$;
(ii) W is a polynomial function of terms that are uncoupled with respect to the invariants $\{I_1,\ I_3,\ I_5,\ I_7\}$; and
(iii) W is at most a quadratic function of the invariant I_7.[1]

The resulting equation is:

$$\begin{aligned}\mathbf{P} = \mathbf{R}\tilde{\mathbf{P}}(\mathbf{E}) = \mathbf{R}\{&\lambda_{11}E_{11}\mathbf{M}_1 + \lambda_{22}E_{22}\mathbf{M}_2\\ &+\lambda_{33}E_{33}\mathbf{M}_3\\ &+\lambda[(E_{22}+E_{33})\mathbf{M}_1 + (E_{11}+E_{33})\mathbf{M}_2\\ &+(E_{11}+E_{22})\mathbf{M}_3] + 2\mu\mathbf{E}\\ &+(1/2)\lambda_{11}E_{11}(\mathbf{E}\mathbf{M}_1 - \mathbf{M}_1\mathbf{E}) + (1/2)\lambda_{22}\\ &\times E_{22}(\mathbf{E}\mathbf{M}_2 - \mathbf{M}_2\mathbf{E})\\ &+(1/2)\lambda_{33}E_{33}(\mathbf{E}\mathbf{M}_3 - \mathbf{M}_3\mathbf{E}) + (1/2)\lambda\\ &\times[(E_{22}+E_{33})(\mathbf{E}\mathbf{M}_1 - \mathbf{M}_1\mathbf{E})\\ &+(E_{11}+E_{33})(\mathbf{E}\mathbf{M}_2 - \mathbf{M}_2\mathbf{E})\\ &+(E_{11}+E_{22})(\mathbf{E}\mathbf{M}_3 - \mathbf{M}_3\mathbf{E})]\\ &+\mu\mathbf{E}^2 + \lambda(\mathbf{I}\cdot\mathbf{E}^2)\mathbf{I} + 2\lambda(\mathbf{I}\cdot\mathbf{E})\mathbf{E}\\ &+\gamma_1(E_{11})^2\mathbf{M}_1 + \gamma_2(E_{22})^2\mathbf{M}_2 + \gamma_3(\mathbf{E}_{33})^2\mathbf{M}_3\}.\end{aligned} \tag{10}$$

[1] These restrictions can be relaxed somewhat because only the corresponding derivatives of W as evaluated in the reference configuration must vanish in the second-order theory.

This model has eight material constants $\{\lambda_{11}, \lambda_{22}, \lambda_{33}, \lambda, \mu, \gamma_1, \gamma_2, \gamma_3\}$, which are defined in terms of the strain energy function W in Appendix B.

2.3 Bimodular elastic materials

Curnier et al. (1995) developed a bimodular theory for linear elastic materials in terms of the second Piola–Kirchhoff stress and Lagrange strain tensors. Here, a bimodular theory for finite deformations is posed in terms of the right stretch tensor $\mathbf{U}$ or, equivalently, the Biot strain tensor $\mathbf{E}$. The elasticity tensors associated with $\hat{\mathbf{P}}(\mathbf{U})$ and $\tilde{\mathbf{P}}(\mathbf{E})$ [defined in $(6)_2$] are defined as

$$P_U = \frac{\partial\hat{\mathbf{P}}(\mathbf{U})}{\partial\mathbf{U}}, \quad P_E = \frac{\partial\tilde{\mathbf{P}}(\mathbf{E})}{\partial\mathbf{E}}, \tag{11}$$

where it can be shown that $P_U(\mathbf{E}+\mathbf{I}) = P_E(\mathbf{E})$. We require the existence of a stress-free reference configuration; i.e., $\hat{\mathbf{P}}(\mathbf{I}) = \tilde{\mathbf{P}}(\mathbf{0}) = \mathbf{0}$. A scalar valued function of $\mathbf{U}$ or $\mathbf{E}$ that identifies a surface of discontinuity in the six-dimensional strain space is defined as

$$g_U(\mathbf{U}) = \mathbf{0}, \quad g_E(\mathbf{E}) = g_U(\mathbf{E}+\mathbf{I}) = \mathbf{0}, \tag{12}$$

where it can be shown that

$$\frac{\partial g_U}{\partial\mathbf{U}}(\mathbf{E}+\mathbf{I}) = \frac{\partial g_E}{\partial\mathbf{E}}(\mathbf{E}). \tag{13}$$

Due to the surface of discontinuity, the stress constitutive equation and, consequently, the elasticity tensor may be different on either side of the surface of discontinuity; here we define

$$\tilde{\mathbf{P}}(\mathbf{E}) = \begin{cases}\tilde{\mathbf{P}}_+(\mathbf{E}) & \text{if } g_E(\mathbf{E}) > 0\\ \tilde{\mathbf{P}}_-(\mathbf{E}) & \text{if } g_E(\mathbf{E}) < 0\end{cases}, \quad P_E = \begin{cases}P_{E+} & \text{if } g_E(\mathbf{E}) > 0\\ P_{E-} & \text{if } g_E(\mathbf{E}) < 0\end{cases}. \tag{14}$$

In Curnier et al. (1995), a theorem that established necessary and sufficient conditions for the stress–strain equation to be continuous across the surface of discontinuity was proved. Here, that theorem is slightly modified, because the major symmetry of the elasticity tensor for linear elastic materials was invoked in Curnier et al. (1995) whereas the elasticity tensor for finitely elastic materials need not possess major symmetry. By not invoking that symmetry assumption, a minor modification of the proof presented in Curnier et al. (1995) leads to the following necessary and sufficient conditions for the stress–strain equation to be continuous across the surface of discontinuity:

$$\begin{aligned}\tilde{\mathbf{P}}(\mathbf{E}) = \tilde{\mathbf{P}}_+(\mathbf{E}) = \tilde{\mathbf{P}}_-(\mathbf{E}), [P_E]] = P_{E+} - P_{E-}\\ = s(\mathbf{E})\mathbf{M}(\mathbf{E}) \otimes \frac{\partial g_E}{\partial\mathbf{E}},\end{aligned} \tag{15}$$

for all $\mathbf{E}$ such that $g_E(\mathbf{E}) = 0$, where $s(\mathbf{E})$ is a scalar valued function and $\mathbf{M}(\mathbf{E})$ is a second-order tensor. [2] Due to material symmetry, the surface of discontinuity must satisfy

$$g_E(\mathbf{E}) = \tilde{g}_U(I_U)\,|_{\mathbf{U}=\mathbf{E}-\mathbf{I}}\,. \tag{16}$$

[2] See Lemma 3.2 in Curnier et al. (1995).

The development in (11)–(15) can be easily modified if one prefers to work with the Cauchy stress. The functions $\hat{\mathbf{T}}(\mathbf{U})$ and $\tilde{\mathbf{T}}(\mathbf{E})$ replace $\hat{\mathbf{P}}(\mathbf{U})$ and $\tilde{\mathbf{P}}(\mathbf{E})$ and the elasticity tensors are defined as in (11); e.g. $T_E = \partial\tilde{\mathbf{T}}(\mathbf{E}) \Big/ \partial\mathbf{E}$.

2.4 Bimodular second-order orthotropic materials

For a second-order elastic material, not all surfaces that satisfy the material symmetry restriction (16) will satisfy the continuity conditions (15). In order to model tension-compression asymmetry along the three directions defining orthotropy, we use three surfaces of discontinuity:

$$\begin{aligned} g_1 &= \mathbf{M}_1 \cdot \mathbf{E} = E_{11} = 0, \\ g_2 &= \mathbf{M}_2 \cdot \mathbf{E} = E_{22} = 0, \\ g_3 &= \mathbf{M}_3 \cdot \mathbf{E} = E_{33} = 0. \end{aligned} \tag{17}$$

Consider the surface $g_1 = 0$. Inspection of the stress constitutive equation for $\mathbf{P}$, i.e. Eq. (10), reveals that the first continuity condition $(15)_1$ (i.e., $\tilde{\mathbf{P}}_+(\mathbf{E}) = \tilde{\mathbf{P}}_-(\mathbf{E})$ for all $\mathbf{E}$ such that $E_{11} = 0$) requires that the only material constants that may jump across this surface are $\{\lambda_{11},\ \gamma_1\}$. We adopt the notation

$$[[\lambda_{11}]] = \lambda_{11+} - \lambda_{11-}, \quad \lambda_{11}[E_{11}] = \begin{cases} \lambda_{11+} & \text{if } E_{11} > 0 \\ \lambda_{11-} & \text{if } E_{11} < 0 \end{cases}. \tag{18}$$

The terms in $\tilde{\mathbf{P}}(\mathbf{E})$ that involve the jump constants are highlighted as follows:

$$\begin{aligned} \tilde{\mathbf{P}}(\mathbf{E}) = \cdots &+ \lambda_{11} E_{11}\mathbf{M}_1 + \frac{1}{2}\lambda_{11} E_{11}(\mathbf{E}\mathbf{M}_1 - \mathbf{M}_1\mathbf{E}) \\ &+ \gamma_1 (E_{11})^2 \mathbf{M}_1 + \cdots \end{aligned} \tag{19}$$

Using (19) and calculating the jump in the elasticity tensor P_{E} using $(11)_2$ we obtain, switching to indicial notation,

$$\begin{aligned} [[P_{\mathrm{E}}]] &= \left[\left[\frac{\partial \tilde{P}_{AB}}{\partial E_{KL}} \right]\right] \\ &= [[\lambda_{11}]] \left\{ \delta_{1A}\delta_{1B}\delta_{1K}\delta_{1L} + \frac{1}{2}\left[E_{12}\left(\delta_{2A}\delta_{1B} - \delta_{1A}\delta_{2B}\right)\right.\right. \\ &\qquad \left.\left. + E_{13}\left(\delta_{3A}\delta_{1B} - \delta_{1A}\delta_{3B}\right)\right]\delta_{1K}\delta_{1L} \right\} \end{aligned} \tag{20}$$

where the condition $E_{11} = 0$ at the interface was used. Furthermore,

$$\frac{\partial g_1}{\partial E_{KL}} = \frac{\partial E_{11}}{\partial E_{KL}} = \delta_{1K}\delta_{1L}, \tag{21}$$

so that the second continuity condition $(15)_2$ becomes

$$[[P_E]] = s(\mathbf{E}) M_{AB}\delta_{1K}\delta_{1L}. \tag{22}$$

Comparison of (20) and (22) reveals that the second continuity condition may be satisfied. Therefore, a bimodular second-order material with a surface of discontinuity defined by $g_1 = E_{11} = 0$ may be represented by replacing the material constants $\{\lambda_{11},\ \gamma_1\}$ with $\{\lambda_{11}[E_{11}],\ \gamma_1[E_{11}]\}$ where we have used the notation of $(18)_2$. Using a similar analysis, or by interchanging the indices appropriately, a bimodular material with additional surfaces of discontinuity $g_2 = E_{22} = 0$ and $g_3 = E_{33} = 0$ may have discontinuous material constants $\{\lambda_{22},\ \gamma_2\}$ and $\{\lambda_{33},\ \gamma_3\}$, respectively. Consequently, the bimodular stress constitutive equation corresponding to the reduced second-order orthotropic material (10) may have a total of 14 material constants. [3] A similar analysis using the Cauchy stress reveals that the same material constants can jump across these surfaces of discontinuity.

Finally, we make two additional simplifying assumptions for the analyses of the present study. First, we require that the first-order constants $\{\lambda_{11},\ \lambda_{22},\ \lambda_{33}\}$ be continuous across the surfaces of discontinuity. The rationale for this requirement is that previous analyses suggested that material stability is difficult to ensure if the first-order constants jump, because eight stiffness matrices must be positive-definite (see, Klisch et al. 2004; Wang et al. 2003). Second, we neglect the second-order terms associated with λ and μ [see Eqs. (10) or (37)]. [4] The rationale for this reduction is that preliminary results for models that included these second-order terms exhibited a non-convex mechanical response in CC. Thus, we consider the reduced model

$$\begin{aligned} \mathbf{P} = \mathbf{R}\tilde{\mathbf{P}}(\mathbf{E}) = \mathbf{R}\{ &\lambda_{11}E_{11}\mathbf{M}_1 + \lambda_{22}E_{22}\mathbf{M}_2 + \lambda_{33}E_{33}\mathbf{M}_3 \\ &+ \lambda[(E_{22} + E_{33})\mathbf{M}_1 + (E_{11} + E_{33})\mathbf{M}_2 \\ &+ (E_{11} + E_{22})\mathbf{M}_3] + 2\mu\mathbf{E} \\ &+ (1/2)\lambda_{11}E_{11}(\mathbf{E}\mathbf{M}_1 - \mathbf{M}_1\mathbf{E}) \\ &+ (1/2)\lambda_{22}E_{22}(\mathbf{E}\mathbf{M}_2 - \mathbf{M}_2\mathbf{E}) \\ &+ (1/2)\lambda_{33}E_{33}(\mathbf{E}\mathbf{M}_3 - \mathbf{M}_3\mathbf{E}) \\ &+ (1/2)\lambda[(E_{22} + E_{33})(\mathbf{E}\mathbf{M}_1 - \mathbf{M}_1\mathbf{E}) \\ &+ (E_{11} + E_{33})(\mathbf{E}\mathbf{M}_2 - \mathbf{M}_2\mathbf{E}) + (E_{11} + E_{22}) \\ &\times(\mathbf{E}\mathbf{M}_3 - \mathbf{M}_3\mathbf{E})] \\ &+ \gamma_1[E_{11}](E_{11})^2\mathbf{M}_1 + \gamma_2[E_{22}](E_{22})^2\mathbf{M}_2 \\ &+ \gamma_3[E_{33}](E_{33})^2\mathbf{M}_3 \big\}, \end{aligned} \tag{23}$$

which results in a maximum of 11 parameters. It is important to emphasize that in (23), only the second-order material constants may jump. Consequently, the elasticity tensor (in addition to the strain energy function and stress–strain equation) is continuous across the surfaces of discontinuity whereas the gradient of the elasticity tensor may jump. Finally, for pure stretch deformations, (23) simplifies to

$$\begin{aligned} \mathbf{P} = \tilde{\mathbf{P}}(\mathbf{E}) = &\lambda_{11}E_{11}\mathbf{M}_1 + \lambda_{22}E_{22}\mathbf{M}_2 + \lambda_{33}E_{33}\mathbf{M}_3 \\ &+ \lambda[(E_{22} + E_{33})\mathbf{M}_1 + (E_{11} + E_{33})\mathbf{M}_2 \\ &+ (E_{11} + E_{22})\mathbf{M}_3] + 2\mu\mathbf{E} \\ &+ \gamma_1[E_{11}](E_{11})^2\mathbf{M}_1 + \gamma_2[E_{22}](E_{22})^2\mathbf{M}_2 \\ &+ \gamma_3[E_{33}](E_{33})^2\mathbf{M}_3. \end{aligned} \tag{24}$$

[3] The bimodular stress constitutive equation corresponding to the general second-order orthotropic material may have a total of 61 material constants.

[4] Consequently, the equation studied is no longer an exact second-order approximation.

Note that we have again used the notation introduced in $(18)_2$ for the discontinuous material constants $\{\gamma_1,\ \gamma_2,\ \gamma_3\}$.

2.5 A bimodular exponential orthotropic material

To compare the predictive capability of (24) with current exponential models, we considered a strain energy function of the form (5):

$$W = \tilde{W}(I_C) = \frac{a_1}{2}[I_7 - (I_7)^{-1}]^2 + \sum_{i=1}^{3} \frac{b_i}{2c_i}\left[e^{c_i(I_i-1)^2} - 1\right], \tag{25}$$

with seven parameters $(a_1, b_1, c_1, b_2, c_2, b_3, c_3)$ where, for convenience, we have ordered the invariants of $\mathbf{C}$ as

$$\begin{aligned}\{I_i(\mathbf{C})\} &= \{\mathbf{M}_1 \cdot \mathbf{C}, \mathbf{M}_2 \cdot \mathbf{C}, \mathbf{M}_3 \cdot \mathbf{C}, \mathbf{M}_1 \cdot \mathbf{C}^2, \mathbf{M}_2 \\ &\quad \cdot \mathbf{C}^2, \mathbf{M}_3 \cdot \mathbf{C}^2, det\mathbf{C}\} \\ &\equiv \{I_1,\ I_2,\ I_3,\ I_4,\ I_5,\ I_6,\ I_7\}. \end{aligned} \tag{26}$$

In (25), the isotropic part (i.e., the term dependent on I_7) was based on the orthotropic model of Wagner and Lotz (2004) while the anisotropic part was based on the study of Holzapfel et al. (2004). Recently, exponential strain energy functions of the type (25) have been employed that are "bimodular" (Baer et al. 2004; Holzapfel et al. 2004). In those studies the anisotropy is attributed to the presence of collagen fibers that are hypothesized to support only tensile stresses. To be consistent with those studies, it suffices to investigate whether the constants b_1, b_2, and b_3 can jump across the surfaces of discontinuity defined by $I_1 = 1$, $I_2 = 1$, and $I_3 = 1$, respectively. First, (4) is used to calculate $\mathbf{P}$, which can then be expressed as $\mathbf{P} = \mathbf{R}\tilde{\mathbf{P}}(\mathbf{E})$. Then, using the methods outlined above, it can be confirmed that the continuity conditions (15) can be satisfied while allowing the constants b_1, b_2, and b_3 to jump across the surfaces $I_1 = 1$, $I_2 = 1$, and $I_3 = 1$, respectively. Thus, to employ the exponential model (25) and to be consistent with Baer et al. (2004) and Holzapfel et al. (2004), we consider $b_1 = 0, b_2 = 0$, and $b_3 = 0$ when $I_1 < 1, I_2 < 1$, and $I_3 < 1$, respectively, resulting in a 7-parameter model.

2.6 Material stability conditions

For analyses using the reduced orthotropic bimodular model (23), necessary and sufficient conditions for material stability are straightforward to derive and apply. Here, we follow the definition and interpretation of incremental stability for the conjugate pair of Biot stress and Biot strain as presented in Ogden (1984). Appendix C outlines the derivation of the following two necessary and sufficient conditions for material stability: (1) the first-order material constants λ_{11}, λ_{22}, λ_{33}, λ, and μ must correspond to a positive-definite stiffness matrix; and (2) the second-order constants, if non-zero, must satisfy $\gamma_{1+} > 0$, $\gamma_{2+} > 0$, $\gamma_{3+} > 0$, $\gamma_{1-} < 0$, $\gamma_{2-} < 0$, and $\gamma_{3-} < 0$. Stability restrictions are difficult to obtain and verify when using an exponential strain energy function such as (25). In Wagner et al. (2002), it was noted that $a_1 > 0$ is necessary for having a positive definite strain energy function. In Holzapfel et al. (2004), it was argued that $b_i > 0$ is a sufficient condition for strong ellipticity. Thus, these relations are sufficient for incremental stability.

2.7 Experimental data

We constructed a hypothetical experimental dataset (Table 1) that may approximate the mechanical response of adult human cartilage in the surface region, which typically exhibits the strongest anisotropy. The data corresponded to UT and CC experiments along three directions: (1) parallel to the split line, (2) perpendicular to the split line and parallel to the surface, and (3) perpendicular to the surface (Fig. 1). To develop the UT datasets, a 2-parameter exponential function was used to generate data from 0 to 20% strain in 2% increments. For UT in the 1 and 2 directions, the parameters were adopted from Huang et al. (1999, 2005). For UT in the 3 direction, the parameters from the UT in the 1-direction were scaled down using a ratio of the infinitesimal Young's moduli reported in Chahine et al. (2004) for bovine cartilage. Poisson's ratios were assumed to be the same in all three UT experiments, and to be linearly increasing functions of axial strain. The Poisson's ratio at 0% UT strain was assumed to correspond to the Poisson's ratio for infinitesimal deformations in unconfined compression since the stress–strain equation is continuous through the origin, and was chosen using theoretical predictions with bovine tissue (Wang et al. 2003). The Poisson's ratio at 16% strain was specified using the data reported in Huang et al. (1999). To develop the CC datasets, a 2-parameter exponential function (Ateshian et al. 1997) was used to generate data from 0 to 20% strain in 2% increments; the parameters were based on results of Huang et al. (1999, 2005). It was assumed that the CC response was the same in the 1 and 2 directions.

2.8 Regression analysis

A simultaneous nonlinear regression algorithm was performed in Mathematica (Wolfram, V5.0) based on an approach devel-

Table 1 Values of Young's modulus E, Poisson's ratio ν, and aggregate modulus H_A at 0% and 16% strain levels in the 1,2, and 3 directions for the experimental dataset used (E and H_A in MPa)

Parameter	Direction		
	1	2	3
E_0	7.8	5.9	1.2
$E_{0.16}$	42.8	26.3	9.0
ν_0	0.05	0.05	0.05
$\nu_{0.16}$	1.33	1.33	1.33
H_{A0}	0.18	0.18	0.10
$H_{A0.16}$	0.26	0.26	0.15

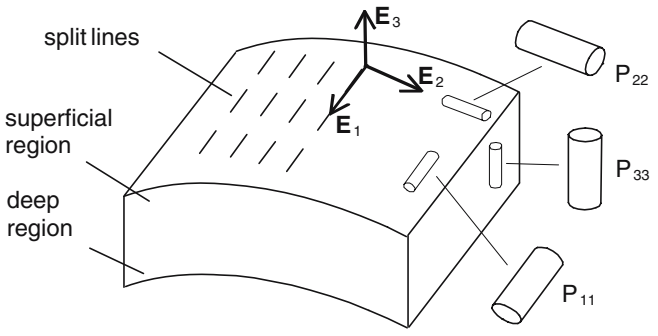

Fig. 1 Schematic diagram of the coordinate system and experimental specimen orientations in relation to anatomical directions. The unit vector $\mathbf{E}_1$ is parallel to the local split-line direction, the unit vector $\mathbf{E}_3$ is perpendicular to the articular surface, and the unit vector $\mathbf{E}_2$ is perpendicular to the split-line direction and parallel to the surface. The cylinders labeled P_{11}, P_{22}, and P_{33} represent specimens loaded in tension or compression along the $\mathbf{E}_1$, $\mathbf{E}_2$, and $\mathbf{E}_3$ directions, respectively

oped by Klisch and Lotz (1999), in which the Levenberg–Marquardt method is used to minimize the sum of squared differences using the theoretical and experimental stress values. Four second-order models were studied, with 6, 7, 8, and 9 parameters (Table 2), and one exponential model was studied, with 7 parameters. The assumed Poisson's functions were used to prescribe the off-axis strains for UT. Then, a composite function representing a total of 12 equations was derived: three axial stress–axial strain equations in CC, three axial stress–axial strain equations in UT, and six transverse stress–axial strain equations in UT (corresponding to the traction-free boundary conditions). The CC stress values were weighted by multiplying each stress value by 100, since the UT stress response is two orders of magnitude greater than the CC stress response. Initial values are required as a starting point for the set of material constants in the regression analysis. When employing the second-order models, the first-order parameters were set to values corresponding to the infinitesimal material constants and the second-order parameters were set equal to zero. When employing the exponential model, initial values were based on those reported in Holzapfel et al. (2004) and Wagner and Lotz (2004).

Table 2 Material parameters in the second-order models studied

Parameter	Model			
	6-PAR	7-PAR	8-PAR	9-PAR
λ_{11}	+	+	+	+
λ_{22}	$=\lambda_{11}$	$=\lambda_{11}$	+	+
λ_{33}	$=\lambda_{11}$	$=\lambda_{11}$	+	+
λ	+	+	+	+
μ	+	+	+	+
γ_{1+}	+	+	+	+
γ_{2+}	+	+	+	+
γ_{3+}	+	+	+	+
γ_{1-}	$=0$	+	$=0$	+
γ_{2-}	$=0$	$=\gamma_{1-}$	$=0$	$=\gamma_{1-}$
γ_{3-}	$=0$	$=\gamma_{1-}$	$=0$	$=\gamma_{1-}$

+ indicates that the material constant was an independent parameter

Preliminary analyses with the second-order models studied revealed non-convexity in the stress–strain response that was accompanied by a violation of the stability criteria. Since the stability restrictions could not be imposed a priori with the numerical algorithm, we formulated a consistent strategy that achieved admissible solutions for each of the models. First, the material constant γ_{1-} was set to a constant value of –0.2 MPa in the 7- and 9-parameter models, corresponding to a value obtained in the preliminary analyses in which the second-order models were applied to the CC data alone (Klisch et al. 2004). Second, the material constant λ was decreased by increments of 0.1 MPa until a positive-definite elasticity tensor was achieved. The exponential model converged to a set of parameters that satisfied the stability restrictions. After the nonlinear regression analysis was performed, the second-order model parameters were used to derive the exact solutions to the CC and UT boundary-value problems, while the exponential model parameters were used to obtain exact and numerical solutions to the CC and UT boundary-value problems, respectively.

3 Results

The numerical values for the material constants for the second-order models are presented in Table 3; the numerical values for the exponential model were $(a_1, b_1, c_1, b_2, c_2, b_3, c_3) = (0.02, 2.66, 3.48, 1.90, 2.90, 0.44, 4.59,$ MPa). The corresponding sum of squares were 9.2, 8.8, 0.8 and 0.3 for the 6-, 7-, 8- and 9-parameter second-order models, respectively, and 8.6 for the exponential model.

Qualitatively, the theoretical predictions of the UT responses were the same for all models, while the theoretical predictions of the CC response and Poisson's ratios were different (Figs. 2–6 and Table 4). In particular, for the second-order models the CC response was linear for the 6- and 8-parameter models because $\gamma_{1-} = \gamma_{2-} = \gamma_{3-} = 0$, nonlinear for the 7- and 9- parameter models because $\gamma_{1-} = \gamma_{2-} = \gamma_{3-} < 0$, equal in all 3 directions for the 6- and 7- parameter models because $\lambda_{11} = \lambda_{22} = \lambda_{33}$, and not equal in all 3 directions for the 8- and 9- parame-

Table 3 Numerical values (MPa) for the material parameters of the second-order models obtained from regression analysis

Parameter	Model			
	6-PAR	7-PAR	8-PAR	9-PAR
λ_{11}	0.091	0.075	0.121	0.106
λ_{22}	0.091	0.075	0.121	0.106
λ_{33}	0.091	0.075	0.03	0.015
λ	0.180	0.140	0.140	0.110
μ	0.045	0.037	0.045	0.038
γ_{1+}	134.1	134.1	133.9	133.9
γ_{2+}	88.1	88.1	87.9	88.0
γ_{3+}	26.4	26.5	26.8	26.8
γ_{1-}	0	−0.2	0	−0.2
γ_{2-}	0	−0.2	0	−0.2
γ_{3-}	0	−0.2	0	−0.2

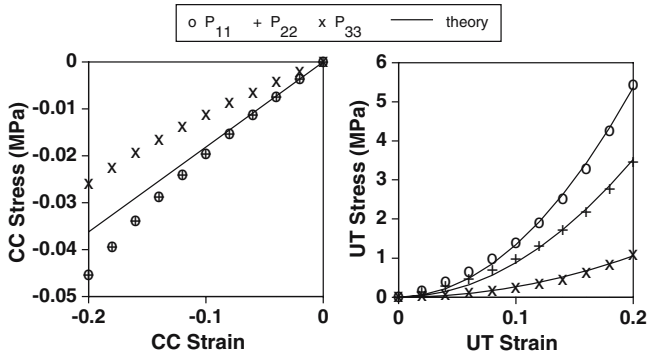

Fig. 2 6-parameter second-order model predictions for the confined compression (CC) response and the uniaxial tension (UT) response. The theoretical CC curves are linear and equal in the 1, 2, and 3 directions

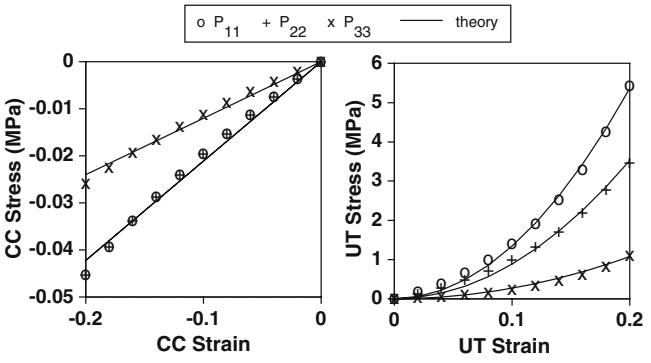

Fig. 4 8-parameter second-order model predictions for the CC response and the UT response. The theoretical CC curves are linear

ter models because $\lambda_{11} = \lambda_{22} \neq \lambda_{33}$. The Poisson's functions were linear for the 6- and 8- parameter models because $\gamma_{1-} = \gamma_{2-} = \gamma_{3-} = 0$, nonlinear for the 7- and 9- parameter models because $\gamma_{1-} = \gamma_{2-} = \gamma_{3-} < 0$, equal in all 3 directions for the 6- and 7- parameter models because $\lambda_{11} = \lambda_{22} = \lambda_{33}$, and not equal in all 3 directions for the 8- and 9- parameter models because $\lambda_{11} = \lambda_{22} \neq \lambda_{33}$. For the exponential model, the CC responses were nonlinear and equal in all 3 directions while the Poisson's functions were nonlinear and equal in all 3 directions.

4 Discussion

In this paper, a bimodular theory for finite deformations was developed with the aim of accurately modeling the orthotropic and asymmetric mechanical response of cartilage. We presented a bimodular orthotropic stress constitutive equation that is second-order in Biot strain, subject to three surfaces of discontinuity, with 14 material constants. Reduced models with 6–9 parameters were proposed and their ability to describe experimental data representative of articular cartilage was assessed. In addition, we studied a 7-parameter bimodular exponential model. Although the 6- and 7-parameter second-order and 7-parameter exponential models provided reasonable fits, they were not capable of modeling the anisotropic CC response and UT Poisson's function. The 8- and 9-parameter second-order models were capable of providing a more accurate description of the anisotropic CC response. These results suggest that the different models studied here may be used in different applications, depending on the relative accuracy desired in the CC and UT responses.

Previous nonlinear orthotropic models for biological tissues had adopted an exponential strain energy function. Lotz and colleagues proposed several exponential strain energy functions for the annulus fibrosus with the aim of obtaining a fit of the experimental data to within one standard deviation of the mean response. In particular, a 9-parameter model was used to fit two UT and two CC experiments (Klisch and Lotz 1999) and a 6-parameter model was used to fit three UT, two CC, one unconfined compression, and one biaxial tension experiment (Wagner and Lotz 2004). Other models for the

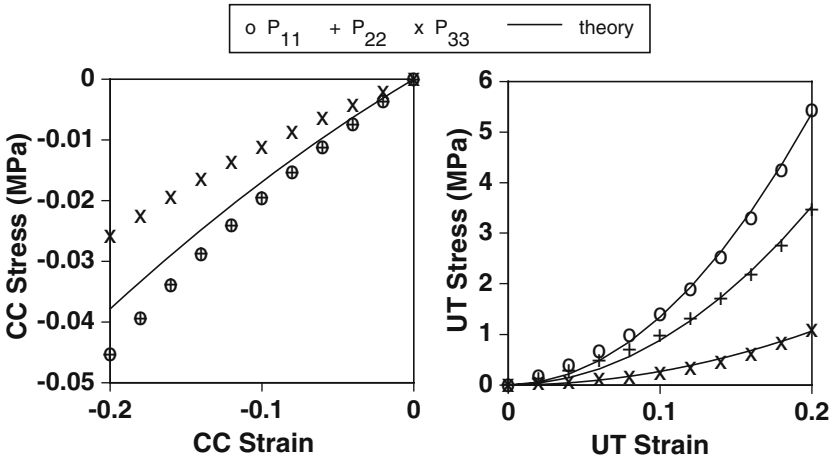

Fig. 3 7-parameter second-order model predictions for the CC response and the UT response. The theoretical CC curves are nonlinear and equal in the 1, 2, and 3 directions

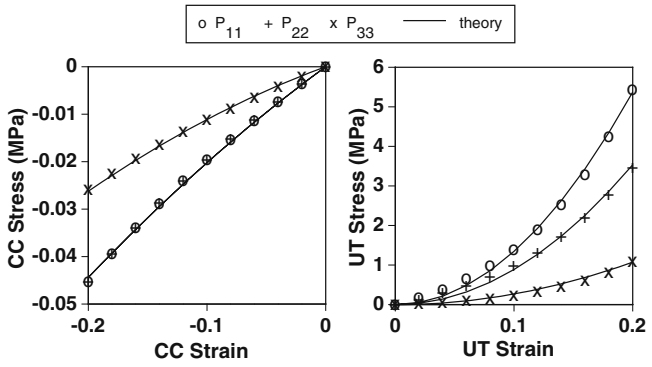

Fig. 5 9-parameter second-order model predictions for the CC response and the UT response. The theoretical CC curves are nonlinear

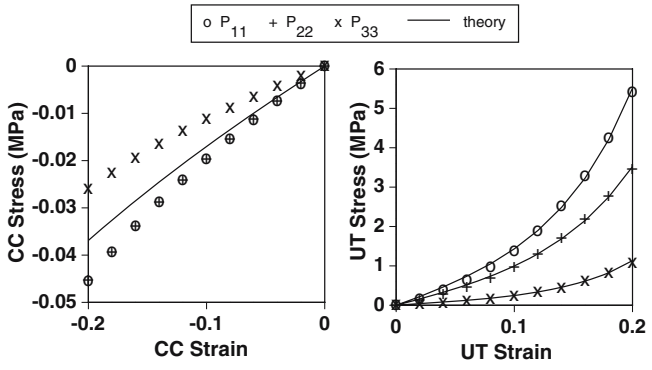

Fig. 6 7-parameter exponential model predictions for the CC response and the UT response. The theoretical CC curves are nonlinear and equal in the 1, 2, and 3 directions

annulus fibrosus include a 3-parameter exponential model that was fit to two UT experiments (Eberlein et al. 2001) and a 6-parameter exponential model with material constants specified to be consistent with published material properties (Baer et al. 2004). For arterial tissue, a 3-parameter exponential model was used to fit a biaxial tension experiment and then predict the response in combined extension and inflation (Holzapfel et al. 2004). For articular cartilage, a stress constitutive equation for finite deformations that can accurately describe the orthotropic and asymmetric mechanical response for multiple experimental protocols has not been proposed. However, bimodular models have been used. As mentioned before, Ateshian and colleagues (Soltz and Ateshian 2000; Wang et al. 2003) used a bimodular model for infinitesimal strains. Also, the orthotropic model proposed for arterial tissue (Holzapfel et al. 2004) and the transversely isotropic model proposed for the intervertebral disc (Baer et al. 2004) allowed for different mechanical properties in tension and compression. Other bimodular models include fiber-reinforced cartilage FEMs in which cable elements, which only support stress under tension, are used to model collagen fibers (Korhonen et al. 2003; Li et al. 1999; Li and Herzog 2004; Soulhat et al. 1999; Wilson et al. 2004).

The bimodular second-order stress constitutive equation has several features that may make it desirable for some applications. First, the use of a second-order equation removes the uncertainty regarding the form of the strain energy function for orthotropic materials as the number of terms and, consequently, the number of material constants is known. However, there is still uncertainty as to which terms need to be retained in order to accurately model the mechanical response. In this study, several simplifying assumptions were invoked in order to obtain an orthotropic second-order stress constitutive equation with only 8 material constants whereas the general equation, which was not presented, has 46 material constants. Second, a systematic procedure for establishing initial guesses for the material constants in a nonlinear regression analysis may be used. Specifically, the first-order constants may be initially set to values obtained using an analysis with infinitesimal strains while the second-order constants may be initially set to zero. Third, the material constants in the second-order equation are straightforward to interpret. From a mathematical perspective, some contants correspond to the infinitesimal theory while the others represent nonlinear (i.e., second-order) effects. Also, the constants do have a physical interpretation; for example, the material constants ($\lambda_{11}, \lambda_{22}, \lambda_{33}, \gamma_1, \gamma_2, \gamma_3$) may reflect the microstructural properties of collagen fibers (e.g., orientation and crosslink density) that give rise to direction-dependent tensile properties. Fourth, the 8- and 9-parameter second-order models studied here provide a reasonable description of the anisotropic responses in both CC and UT.

In each of the bimodular second-order models studied here, the elasticity tensor is continuous through the origin in strain space since only the second-order constants jump across the surfaces of discontinuity. A justification for not allowing the first-order constants to jump is that the experimental stress–strain response is continuous through the origin in strain space, as demonstrated for the annulus fibrosus (Wagner and Lotz 2004) and articular cartilage (Chahine et al. 2004). Consequently, at first it appeared that the material stability criteria for these models are fairly easy to implement. Since the first-order constants may not jump, one stiffness matrix must be checked for positive definiteness, as compared to a maximum of eight if these constants are allowed to jump. In a preliminary study (Klisch et al. 2004), we found that ensuring positive definiteness of eight stiffness matrices

Table 4 Average values of Poisson's ratios ν_{ij} (i=loading direction, j=direction of transverse strain component) predicted for the models (calculated at 20% strain)

	Model				
Parameter	6-PAR	7-PAR	8-PAR	9-PAR	EXP
ν_{12}	0.499	0.46	−0.49	0.13	0.44
ν_{13}	0.499	0.46	1.74	0.79	0.44
ν_{21}	0.499	0.46	−0.49	0.13	0.44
ν_{23}	0.499	0.46	1.74	0.79	0.44
ν_{31}	0.499	0.46	0.40	0.36	0.44
ν_{32}	0.499	0.46	0.40	0.36	0.44

Poisson's ratios were constant for the 6-PAR and 8-PAR models but not for the other models. Note that a constant Poisson's ratio corresponds to a linear Poisson's function

may be overly challenging (see also the discussion in Wang et al. 2003). However, the results of the present study revealed that the numerical regression algorithm did not initially converge to a positive-definite stiffness matrix for the second-order models. This is a limitation of the second-order models as compared to the exponential model (which did converge to a stable solution), although this may be overcome by using a numerical regression algorithm that allows for the a priori specification of bounds on the material constants.

Another limitation of the present study is the uncertainty regarding the theoretical Poisson's ratios that are presented in Table 4. For example, in Huang et al. (1999) the Poisson's ratios measured at 16% strain for UT in the 1 and 2 directions were 1.31 and 1.33, respectively, whereas the 6-parameter second-order model here resulted in constant Poisson's ratios of 0.499. In contrast to earlier studies with exponential strain energy functions (Klisch and Lotz 1999; Wagner and Lotz 2004), in this study an exact solution to UT can be obtained for the second-order models. The stress–strain curves for the exact solutions were nearly identical to those obtained in the nonlinear regression; consequently, the uncertainties in the Poisson's ratios do not seem to affect the models' ability to describe the UT stresses. However, errors may be introduced when extrapolating to the biaxial stress states.

Additional limitations of the present study are concerned with the assumed experimental dataset, as different results can be expected for different datasets. The data used did not correspond to a complete set of UT and CC experiments for a specific source of articular cartilage (i.e., anatomic site, species, age, etc.); however, it did describe a highly orthotropic and asymmetric mechanical response that is typical of cartilage. Also, torsional shear properties were not considered primarily because we have not developed a boundary-value problem solution corresponding to combined torsion and compression (which is commonly used in torsional shear experiments on articular cartilage). The material constant μ that was obtained in the regression analyses corresponded to a shear modulus that was lower, but on the same order of magnitude, than the reported values for articular cartilage (Mow and Ratcliffe 1997). This discrepancy may be partly due to the experimental compression applied during torsional shear. To address these limitations, a current aim of ours is to develop a finite element model using the bimodular theory proposed here and to experimentally measure the mechanical properties for a specific source of articular cartilage in unconfined compression, torsional shear, CC, and UT.

It is important to note that the present approach is phenomenological. Microstructural models have the advantage that they offer a structure–function relationship that relates the tissue's microstructure to the macroscopically observed mechanical properties. For example, experiments with healthy and osteoarthritic cartilage explants have shown that osteoarthritis is accompanied by an increase in tissue hydration and a decrease in proteoglycans (Maroudas 1976), leading to the hypothesis that increased collagen damage is the primary mechanism for swelling (Basser et al. 1998). That hypothesis is based on a stress- balance assumption: in equilibrium, the collagen tensile stress balances the swelling pressure produced by the fixed charge density (Bank et al. 1997; Maroudas 1976). The fiber-reinforced FEMs are microstructural models that employ the stress-balance hypothesis; indeed, the results of one study led to the claim that modeling the tension–compression nonlinearity using separate elements for the collagen and proteoglycan constituents is needed to accurately model the mechanical behavior of normal and degraded cartilage (Korhonen et al. 2003). However, microstructural models typically aim to describe the general features of the tissue's mechanical response (at least in the realm of large strains) and not to accurately fit data from multiple experimental protocols performed on the same specimen.

Phenomenological models have a role in developing accurate biomechanical models. Our approach has been to first develop a phenomenological model, since we believe that phenomenological models may result in more accuracy, [5] and then to incorporate microstructural considerations. We have recently decomposed the solid matrix stress constitutive equation into proteoglycan and collagen stress equations. In particular, in Bingham et al. (2005) a microstructural model first proposed in Basser et al. (1998) and further developed in Klisch et al. (2003) was used to develop a proteoglycan stress equation with material constants that depend on the masses of the tissue constituents (i.e., proteoglycans, collagens, and water) while the 6-parameter bimodular model presented here is used for the collagen stress equation.

Acknowledgements I would like to thank Mrs. Suzanne Holtrichter for assistance in developing the program used in the regression analysis. This material is based upon work supported by the National Science Foundation under Grant No. 0245709, the Office of Naval Research (Department of Navy), and the Donald E. Bently Center for Engineering Innovation.

Appendix A: second-order elastic materials

For an arbitrary material symmetry group, Hoger (1999) derived general stress constitutive equations that are second-order in terms of the Biot strain tensor. That approach used functions $\hat{\mathbf{T}}(\mathbf{U})$ and $\hat{\mathbf{P}}(\mathbf{U})$ derived from $\hat{\mathbf{W}}(\mathbf{U})$ and the truncated series expansion for the gradient of $\hat{\mathbf{W}}(\mathbf{U})$. [6] The derived second-order stress equations are

$$\mathbf{T} = \mathbf{R}\{\Psi_1[\mathbf{E}] + \mathrm{sym}(\mathbf{E}\Psi_1[\mathbf{E}]) - (\mathrm{tr}\mathbf{E})\Psi_1[\mathbf{E}] + \frac{1}{2}\Psi_2[\mathbf{E},\mathbf{E}]\}\mathbf{R}^T,$$

$$\mathbf{P} = \mathbf{R}\{\Psi_1[\mathbf{E}] + \mathrm{skw}(\mathbf{E}\Psi_1[\mathbf{E}]) + \frac{1}{2}\Psi_2[\mathbf{E},\mathbf{E}]\}, \tag{27}$$

where $\mathrm{tr}(\cdot)$ is the trace operator, $\mathrm{sym}(\cdot)$ and $\mathrm{skw}(\cdot)$ are the symmetric and skew parts of a tensor, and

$$\Psi_1[\mathbf{E}] = D\frac{\partial \hat{W}}{\partial \mathbf{U}}(\mathbf{I})[\mathbf{E}] = \frac{\partial^2 W}{\partial I_k \partial I_j}(I_I)\frac{\partial I_j}{\partial \mathbf{U}}(\mathbf{I})\left\{\frac{\partial I_k}{\partial \mathbf{U}}(\mathbf{I})\cdot\mathbf{E}\right\} + \frac{\partial W}{\partial I_j}(I_I)\frac{\partial^2 I_j}{\partial \mathbf{U}^2}(\mathbf{I})[\mathbf{E}],$$

[5] For example, see the discussion on molecular and phenomenological models of rubber elasticity presented in Chapter 7 of Ogden (1984).

[6] See Eq. 2.27–2.28 and 3.3 in (Hoger 1999).

$$\Psi_2[\mathbf{E},\mathbf{E}] = D^2\frac{\partial \hat{W}}{\partial \mathbf{U}}(\mathbf{I})[\mathbf{E},\mathbf{E}]$$
$$= \frac{\partial^3 W}{\partial I_p \partial I_k \partial I_j}(I_I)\left\{\frac{\partial I_p}{\partial \mathbf{U}}(\mathbf{I})\cdot\mathbf{E}\right\}\left\{\frac{\partial I_k}{\partial \mathbf{U}}(\mathbf{I})\cdot\mathbf{E}\right\}\frac{\partial I_j}{\partial \mathbf{U}}(\mathbf{I})$$
$$+2\frac{\partial^2 W}{\partial I_k \partial I_j}(I_I)\left\{\frac{\partial^2 I_j}{\partial \mathbf{U}^2}(\mathbf{I})[\mathbf{E}]\right\}\left\{\frac{\partial I_k}{\partial \mathbf{U}}(\mathbf{I})\cdot\mathbf{E}\right\}$$
$$+\frac{\partial^2 W}{\partial I_k \partial I_j}(I_I)\frac{\partial I_j}{\partial \mathbf{U}}(\mathbf{I})\left\{\mathbf{E}\cdot\frac{\partial^2 I_k}{\partial \mathbf{U}^2}(\mathbf{I})[\mathbf{E}]\right\}$$
$$+\left\{\frac{\partial W}{\partial I_j}(I_I)\right\}D\left\{\frac{\partial^2 I_j}{\partial \mathbf{U}^2}(\mathbf{I})[\mathbf{E}]\right\}[\mathbf{E}]. \tag{28}$$

Notation I_I signifies that the set $\{I_i(\mathbf{U});\, i=1,n\}$ is to be evaluated at $\mathbf{U}$=$\mathbf{I}$ (i.e., in the reference configuration). Standard formulae are used to calculate the derivatives that appear in (28), (e.g., see Gurtin 1984 and Hoger 1999). Here, only the definition of a tensor derivative is presented in order to clarify the notation of (28). Let $\mathbf{Z}=\hat{\mathbf{Z}}(\mathbf{X})$ be a tensor valued function of a tensor $\mathbf{X}$. Then $\mathbf{Z}$ is differentiable at $\mathbf{X}$ if there exists a linear mapping $\mathrm{D}\hat{\mathbf{Z}}(\mathbf{X})$ (i.e., the derivative of $\mathbf{Z}$ at $\mathbf{X}$) such that

$$\hat{\mathbf{Z}}(\mathbf{X}+\mathbf{Y}) = \hat{\mathbf{Z}}(\mathbf{X}) + D\hat{\mathbf{Z}}(\mathbf{X})[\mathbf{Y}] + \mathrm{o}(\mathbf{Y}) \quad \text{as} \quad \mathbf{Y}\to\mathbf{0}, \tag{29}$$

where, introducing the norm operator $|\cdot|$,

$$\tilde{\mathbf{Z}}(\mathbf{Y}) = \mathrm{o}(\mathbf{Y}) \quad \text{if} \lim_{\mathbf{Y}\to 0}\frac{\left|\tilde{\mathbf{Z}}(\mathbf{X})\right|}{|\mathbf{X}|} = \mathbf{0}. \tag{30}$$

If $\mathbf{Z}$ is differentiable at $\mathbf{X}$, then standard formulae can be used to calculate $D\hat{\mathbf{Z}}(\mathbf{X})$ and $D\hat{\mathbf{Z}}(\mathbf{X})[\mathbf{Y}]$; this latter expression is sometimes referred to as the directional derivative of $\mathbf{Z}$ at $\mathbf{X}$ in the direction of $\mathbf{Y}$.

Appendix B: second-order orthotropic materials

Here, we outline the derivation of the stress constitutive equation for second-order orthotropic materials. Recall the set of invariants that we use for orthotropic materials:

$$\{I_i(\mathbf{U})\} = \{\mathbf{M}_1\cdot\mathbf{U}, \mathbf{M}_1\cdot\mathbf{U}^2, \mathbf{M}_2\cdot\mathbf{U}, \mathbf{M}_2\cdot\mathbf{U}^2, \mathbf{M}_3\cdot\mathbf{U}, \mathbf{M}_3\cdot\mathbf{U}^2, \mathbf{I}\cdot\mathbf{U}^3\}$$
$$\equiv \{I_1,\ I_2,\ I_3,\ I_4,\ I_5,\ I_6,\ I_7\}, \tag{31}$$

where the structural tensors $(\mathbf{M}_1, \mathbf{M}_2, \mathbf{M}_3)$ are defined in (8); e.g., $\mathbf{M}_1 = \mathbf{E}_1\otimes\mathbf{E}_1$. A straightforward calculation leads to

$$\left\{\frac{\partial I_i}{\partial \mathbf{U}}(\mathbf{U})\right\} = \{\mathbf{M}_1,\ \mathbf{M}_1\mathbf{U}+\mathbf{U}\mathbf{M}_1,\ \mathbf{M}_2,\ \mathbf{M}_2\mathbf{U}+\mathbf{U}\mathbf{M}_2,$$
$$\mathbf{M}_3,\ \mathbf{M}_3\mathbf{U}+\ \mathbf{U}\mathbf{M}_3,\ 3\mathbf{U}^2\}; \tag{32}$$

consequently,

$$\left\{\frac{\partial I_i}{\partial \mathbf{U}}(\mathbf{I})\right\} = \{\mathbf{M}_1,\ 2\mathbf{M}_1,\ \mathbf{M}_2,\ 2\mathbf{M}_2,\ \mathbf{M}_3,\ 2\mathbf{M}_3,\ 3\mathbf{I}\}. \tag{33}$$

Using standard formulae, we obtain

$$\left\{\frac{\partial^2 I_i}{\partial \mathbf{U}^2}(\mathbf{I})[\mathbf{E}]\right\} = \left\{D\frac{\partial I_i}{\partial \mathbf{U}}(\mathbf{I})[\mathbf{E}]\right\} \tag{34}$$
$$= \{\mathbf{0}, \mathbf{M}_1\mathbf{E}+\ \mathbf{E}\mathbf{M}_1, \mathbf{0}, \mathbf{M}_2\mathbf{E}+\ \mathbf{E}\mathbf{M}_2, \mathbf{0}, \mathbf{M}_3\mathbf{E}+\ \mathbf{E}\mathbf{M}_3, 6\mathbf{E}\},$$

and

$$\left\{D\left\{\frac{\partial^2 I_i}{\partial \mathbf{U}^2}(\mathbf{I})[\mathbf{E}]\right\}[\mathbf{E}]\right\} = \frac{\partial^2\left(\partial I_i/\partial \mathrm{U}_{pq}\right)}{\partial \mathrm{U}_{kl}\partial \mathrm{U}_{mn}}(\mathbf{I})E_{kl}E_{mn}\mathbf{E}_p\otimes\mathbf{E}_q$$
$$= \{\mathbf{0},\mathbf{0},\mathbf{0},\mathbf{0},\mathbf{0},\mathbf{0},6\mathbf{E}^2\}. \tag{35}$$

Using the results (33–35) in (28) and, consequently, (27) yields the most general orthotropic second-order stress constitutive equations in terms of the Biot strain tensor. This equation has a total of 46 material constants and is not presented here.

However, the stress constitutive equation reduces considerably due to the assumptions stated in the text. In particular, the partial derivatives W_2, W_4, W_6, $W_{ij}(i\neq j)$, and W_{777} are all identically zero and only eight material constants survive. Consequently, we obtain the following results:

$$\Psi_1[\mathbf{E}] = \lambda_{11}E_{11}\mathbf{M}_1 + \lambda_{22}E_{22}\mathbf{M}_2 + \lambda_{33}E_{33}\mathbf{M}_3$$
$$+\lambda[(E_{22}+E_{33})\mathbf{M}_1 + (E_{11}+E_{33})\mathbf{M}_2$$
$$+(E_{11}+E_{22})\mathbf{M}_3] + 2\mu\mathbf{E} \tag{36}$$

and

$$\frac{1}{2}\Psi_2[\mathbf{E},\mathbf{E}] = \mu\mathbf{E}^2 + \lambda(\mathbf{I}\cdot\mathbf{E}^2)\mathbf{I} + 2\lambda(\mathbf{I}\cdot\mathbf{E})\mathbf{E}$$
$$+\gamma_1(E_{11})^2\mathbf{M}_1 + \gamma_2(E_{22})^2\mathbf{M}_2 + \gamma_3(E_{33})^2\mathbf{M}_3. \tag{37}$$

The eight material constants in (36) and (37) are defined as follows, where the subscripts refer to the partial derivative of W with respect to the corresponding invariant $I_i(U)$:

$$\lambda_{11} = W_{11}+9W_{77},\quad \lambda_{22} = W_{33}+9W_{77},\quad \lambda_{33} = W_{55}+9W_{77},$$
$$\lambda = 9W_{77},\quad \mu = 3W_7,\quad \gamma_1 = 2W_{111},\quad \gamma_2 = 2W_{333},\quad \gamma_3 = 2W_{555}. \tag{38}$$

It is emphasized that all partial derivatives of W are evaluated in the reference configuration. These equations can then be used in (27) and (28) to obtain orthotropic second-order stress constitutive equations in terms of either $\mathbf{T}$ or $\mathbf{P}$ [the equation for $\mathbf{P}$ is presented in Eq. (10)].

Appendix C: material stability conditions

A growing number of studies on the material stability of elastic materials have required that the strain energy function be polyconvex (e.g., see, Schroder et al. 2005). However, the strain energy function for the second-order model studied here does not need to be known, as the material constants are defined as derivatives of the strain energy function (with respect to the invariants) and evaluated in the reference configuration. Consequently, it is advantageous to identify conditions for material stability that are posed in terms of the stress constitutive equation. Here, we follow the definition and interpretation of incremental stability for the conjugate pair of Biot stress and Biot strain as presented in Ogden

(1984) and derive necessary and sufficient material stability conditions for the reduced orthotropic bimodular second-order model (23). The Biot stress tensor $\mathbf{T}^{(1)}$ is defined as

$$\mathbf{T}^{(1)} = (1/2)(\mathbf{P}^T\mathbf{R} + \mathbf{R}^T\mathbf{P}). \tag{39}$$

Here, $\mathbf{T}^{(1)}$ corresponds to the symmetric part of $\tilde{\mathbf{P}}(\mathbf{E})$ defined by (23); consequently, $\mathbf{T}^{(1)}(\mathbf{E})$ is equivalent to $\tilde{\mathbf{P}}(\mathbf{E})$ for pure stretches as given in (24). By using (24) to calculate the elasticity tensor P_E and additively decomposing it as $P_E = P_{E1} + P_{E2}$ such that P_{E1} contains the first-order terms and P_{E2} contains the second-order terms, the stability criterion becomes

$$\mathrm{tr}\{(P_{E1}\dot{\mathbf{E}})\dot{\mathbf{E}}\} + \mathrm{tr}\{(P_{E2}\dot{\mathbf{E}})\dot{\mathbf{E}}\} > 0 \quad \text{for all } \dot{\mathbf{E}} \neq 0. \tag{40}$$

In Ogden (1984) [7], this inequality is interpreted as stability "under tractions which follow the material, i.e. rotate with the local rotation $\mathbf{R}$ ... for an isotropic material." It is easy to show that this interpretation extends to the second-order orthotropic material $\mathbf{P} = \mathbf{R}\tilde{\mathbf{P}}(\mathbf{E})$.

To obtain the necessary conditions, first consider stability at zero strain. Then, P_{E2}=$\mathbf{0}$ and (40) reduces to $\mathrm{tr}\{(P_{E1}\dot{\mathbf{E}})\dot{\mathbf{E}}\} > 0$ for all $\dot{\mathbf{E}} \neq 0$, leading to the condition that P_{E1} must be positive-definite; i.e., the first-order material constants λ_{11}, λ_{22}, λ_{33}, λ, and μ must correspond to a positive-definite stiffness matrix. Then, noting that for a fixed $\dot{\mathbf{E}}$ the numerical value of $\mathrm{tr}\{(P_{E1}\dot{\mathbf{E}})\dot{\mathbf{E}}\}$ is finite and positive, consideration of a strain state $\mathbf{E}$ with arbitrarily large magnitude leads to the condition that $\mathrm{tr}\{(P_{E2}\dot{\mathbf{E}})\dot{\mathbf{E}}\} > 0$ for all $\dot{\mathbf{E}} \neq 0$, where $\mathrm{tr}\{(P_{E2}\dot{\mathbf{E}})\dot{\mathbf{E}}\} > 0$ is

$$2\gamma_1 E_{11}(\dot{E}_{11})^2 + 2\gamma_2 E_{22}(\dot{E}_{22})^2 + 2\gamma_3 E_{33}(\dot{E}_{33})^2 > 0. \tag{41}$$

First, consider the special case where $\dot{E}_{22} = \dot{E}_{33} = 0$. Then, $E_{11} > 0$ implies that $\gamma_1 > 0$ and $E_{11} < 0$ implies that $\gamma_1 < 0$. Consequently, for each of the second-order constants that are non-zero, the inequality (41) then leads to the necessary conditions that $\gamma_{1+} > 0$, $\gamma_{2+} > 0$, $\gamma_{3+} > 0$, $\gamma_{1-} < 0$, $\gamma_{2-} < 0$, $\gamma_{3-} < 0$. Sufficiency follows easily.

It is interesting to note that the necessary conditions arising from (41) lead to the requirement that if one adopts the reduced second-order model (23) with any of the second-order constants $\{\gamma_1, \gamma_2, \gamma_3\}$ non-zero, then our assumed stability criterion requires that the material be bimodular. See the related result and discussion following Eq. (28) in Holzapfel et al. (2004), where for their bimodular model it was noted that "strong ellipticity is therefore consistent with fibre extension, which was anticipated ...".

References

Akizuki S, Mow VC, Muller F, Pita JC, Howell DS, Manicourt DH (1986) Tensile properties of human knee joint cartilage: I. Influence of ionic conditions, weight bearing, and fibrillation on the tensile modulus. J Orthop Res 4:379–392

Almeida ES, Spilker RL (1997) Mixed and penalty finite element models for the nonlinear behavior of biphasic soft tissues in finite deformation. Part i-alternative formulations. Comput Methods Biomech Biomed Eng 1:25–46

Ateshian GA, Warden WH, Kim JJ, Grelsamer RP, Mow VC (1997) Finite deformation biphasic material properties of bovine articular cartilage from confined compression experiments. J Biomech 30:1157–1164

Baer AE, Laursen TA, Guilak F, Setton LA (2004) The micromechanical environment of intervertebral disc cells determined by a finite deformation, anisotropic, and biphasic finite element model. J Biomech Eng 125:1–11

Bank RA, Krikken M, Beekman B, Stoop R, Maroudas A, Lafeber FPJG, Te Koppele JM (1997) A simplified measurement of degraded collagen in tissues: Application in healthy, fibrillated and osteoarthritic cartilage. Matrix Biol 16:233–243

Basser PJ, Schneiderman R, Bank RA, Wachtel E, Maroudas A (1998) Mechanical properties of the collagen network in human articular cartilage as measured by osmotic stress technique. Arch Biochem Biophys 351:207–219

Bingham M, Davol A, Sah RL, Klisch SM (2005) A nonlinear finite element model of cartilage growth under in vitro dynamic compression. ASME summer bioengineering conference

Chahine NO, Wang CC, Hung CT, Ateshian GA (2004) Anisotropic strain-dependent material properties of bovine articular cartilage in the transitional range from tension to compression. J Biomech 37:1251–1261

Curnier A, He QC, Zysset P (1995) Conewise linear elastic materials. J Elast 37:1–38

Donzelli PS, Spilker RL, Ateshian GA, Mow VC (1999) Contact analysis of biphasic transversely isotropic cartilage layers and correlations with tissue failure. J Biomech 32:1037–1047

Eberlein R, Holzapfel GA, Schulze-Bauer CA (2001) An anisotropic constitutive model for annulus tissue and enhanced finite element analyses of intact lumbar disc bodies. Comp Meth Biomech Biomed Eng 4:209–230

Eckstein F, Lemberger B, Stammberger T, Englmeier KH, Reiser M (2000) Patellar cartilage deformation in vivo after static versus dynamic loading. J Biomech 33:819–825

Guilak F, Mow VC (2000) The mechanical environment of the chondrocyte:A biphasic finite element model of cell-matrix interactions in articular cartilage. J Biomech 33:1663–1673

Gurtin M (1984) Introduction to continuum mechanics. Academic Press, New York

Herberhold C, Faber S, Stammberger T, Steinlechner M, Putz R, Englmeier KH, Reiser M, Eckstein F (1999) In situ measurement of articular cartilage deformation in intact femoropatellar joints under static loading. J Biomech 32:1287–1295

Hoger A (1999) A second order constitutive theory for hyperelastic materials. Int J Solids Struct 36:847–868

Holmes MH, Mow VC (1990) The nonlinear characteristics of soft gels and hydrated connective tissue in ultrafiltration. J Biomech 23:1145–1156

Holzapfel GA, Gasser TC, Ogden RW (2004) Comparison of a multilayer structural model for arterial walls with a fung-type model, and issues of material stability. J Biomech Eng 126:264–275

Huang CY, Stankiewicz A, Ateshian GA, Flatow EL, Bigliani LU, Mow VC (1999) Anisotropy, inhomogeneity, and tension-compression nonlinearity of human glenohumeral cartilage in finite deformation. Trans Orthop Res Soc (in press)

Huang CY, Stankiewicz A, Ateshian GA, Mow VC (2005) Anisotropy, inhomogeneity, and tension-compression nonlinearity of human glenohumeral cartilage in finite deformation. J Biomech 38:799–809

Klisch SM, Hoger A (2003) Volumetric growth of thermoelastic materials and mixtures. Math Mech Solids 8:377–402

Klisch SM, Lotz JC (1999) Application of a fiber-reinforced continuum theory to multiple deformations of the annulus fibrosus. J Biomech 32:1027–1036

Klisch SM, Sah RL, Hoger A (2000) A growth mixture theory for cartilage. In: Casey J, Bao G (ed) Mechanics in biology. AMB 242 and BED 46, ASME

Klisch SM, Van Dyke T, Hoger A (2001) A theory of volumetric growth for compressible elastic materials. Math Mech Solids 6:551–575

[7] See Eq. (6.2.211) and footnote on pg. 407 of Ogden (1984).

Klisch SM, Chen SS, Sah RL, Hoger A (2003) A growth mixture theory for cartilage with applications to growth-related experiments on cartilage explants. J Biomech Eng 125:169–179
Klisch SM, Holtrichter SE, Sah RL, Davol A (2004) A bimodular second-order orthotropic stress constitutive equation for cartilage. Proceedings of IMECE (ASME)
Klisch SM, Sah RL, Hoger A (2005) A cartilage growth mixture model for infinitesimal strains: Solutions of boundary-value problems related to in vitro growth experiments. Biomech Model Mechanobiol 3:209–223
Korhonen RK, Laasanen MS, Toyras J, Lappalainen R, Helminen HJ, Jurvelin JS (2003) Fibril reinforced poroelastic model predicts specifically mechanical behavior of normal, proteoglycan depleted and collagen degraded articular cartilage. J Biomech 36:1373–1379
Krishnan R, Park S, Eckstein F, Ateshian GA (2003) Inhomogeneous cartilage properties enhance superficial insterstitial fluid support and frictional properties, but do not provide a homogeneous state of stress. J Biomech Eng 125:569–577
Kwan MK, Lai WM, Mow VC (1990) A finite deformation theory for cartilage and other soft hydrated connective tissues – i. Equilibrium results. J Biomech 23:145–155
Laasanen M, Toyras J, Korhonen R, Rieppo J, Saarakkala S, Nieminen M, Hirvonen J, Jurvelin JS (2003) Biomechanical properties of knee articular cartilage. Biorheology 40:133–140
Lai WM, Hou JS, Mow VC (1991) A triphasic theory for the swelling and deformation behaviors of articular cartilage. J Biomech Eng 113:245–258
Li LP, Herzog W (2004) Strain-rate dependence of cartilage stiffness in unconfined compression: The role of fibril reinforcement versus tissue volume change in fluid pressurization. J Biomech 37:375–382
Li L, Soulhat J, Buschmann MD, Shirazi-Adl A (1999) Nonlinear analysis of cartilage in unconfined ramp compression using a fibril reinforced poroelastic model. Clin Biomechanics 14:673–682
Maroudas A (1976) Balance between swelling pressure and collagen tension in normal and degenerate cartilage. Nature 260:808–809
Mow VC, Ratcliffe A (1997) Structure and function of articular cartilage and meniscus. In: Mow VC, Hayes WC (ed) Basic orthopaedic biomechanics. Raven Press, New York
Murnaghan FD (1937) Finite deformation of an elastic solid. Amer J Math 59:235–260
Murnaghan FD (1951) Finite deformation of an elastic solid. Dover, New York
Ogden RW (1984) Non-linear elastic deformations. Dover, Mineola, New York
Rivlin RS (1953) The solution of problems in second order elasticity theory. J Ration Mech Anal 2:53–81
Schinagl RM, Gurskis D, Chen AC, Sah RL (1997) Depth-dependent confined compression modulus of full-thickness bovine articular cartilage. J Orthop Res 15:499–506
Schroder J, Neff P, Balzani D (2005) A variational approach for materially stable anisotropic hyperelasticity. Int J Solids Struct 42:4352–4371
Soltz MA, Ateshian GA (2000) A conewise linear elasticity mixture model for the analysis of tension–compression nonlinearity in articular cartilage. J Biomech Eng 122:576–586
Soulhat J, Buschmann MD, Shirazi-Adl A (1999) A fibril-network-reinforced biphasic model of cartilage in unconfined compression. J Biomech Eng 121:340–347
Van Dyke TJ, Hoger A (2000) A comparison of second-order constitutive theories for hyperelastic materials. Int J Solids Struct 37:5873–5917
Venn MF, Maroudas A (1977) Chemical composition and swelling of normal and osteoarthritic femoral head cartilage. I. Chemical composition. Ann Rheum Dis 36:121–129
Wagner DR (2002) A mechanistic strain energy function and experimental results for the human annulus fibrosus. U.C. Berkeley Ph.D. dissertation
Wagner DR, Lotz JC (2004) Theoretical model and experimental results for the nonlinear elastic behavior of human annulus fibrosus. J Orthop Res 22:901–909
Wang CC-B, Hung CT, Mow VC (2001) An analysis of the effects of depth-dependent aggregate modulus on articular cartilage stress-relaxation behavior in compression. J Biomech 34:75–84
Wang CC, Chahine NO, Hung CT, Ateshian GA (2003) Optical determination of anisotropic material properties of bovine articular cartilage in compression. J Biomech 36:339–353
Wilson W, van Donkelaar CC, van Rietbergen B, Ito K, Huiskes R (2004) Stresses in the local collagen network of articular cartilage: a poroviscoelastic fibril-reinforced finite element study. J Biomech 37:357–366
Woo SL-Y, Akeson WH, Jemmott GF (1976) Measurements of nonhomogeneous directional mechanical properties of articular cartilage in tension. J Biomech 9:785–791
Woo SL-Y, Lubock P, Gomez MA, Jemmott GF, Kuei SC, Akeson WH (1979) Large deformation nonhomogeneous and directional properties of articular cartilage in uniaxial tension. J Biomech 12:437–446